

# Enantio-discrimination via the cavity-assisted three-photon process

Yu-Yuan Chen,<sup>1</sup> Chong Ye,<sup>2,1,\*</sup> and Yong Li<sup>1,3,†</sup>

<sup>1</sup>*Beijing Computational Science Research Center, Beijing 100193, China*

<sup>2</sup>*Beijing Key Laboratory of Nanophotonics and Ultrafine Optoelectronic Systems,  
School of Physics, Beijing Institute of Technology, 100081 Beijing, China*

<sup>3</sup>*Synergetic Innovation Center for Quantum Effects and Applications, Hunan Normal University, Changsha 410081, China*

(Dated: January 19, 2021)

We propose a theoretical method for enantio-discrimination of chiral molecules based on a cavity-molecules system, which consists of a cavity without external driving and an ensemble of chiral mixture (containing left- and right- handed molecules) confined in the cavity. The molecules in the chiral mixture are modeled as cyclic three-level models coupled with the quantized cavity field and two classical light fields. Via the cavity-assisted three-photon process based on the cyclic three-level model, the intracavity photons are generated continuously though there is no external driving to the cavity, and the fields of the photons generated from the left- and right- handed molecules differ with the phase difference  $\pi$ . This provides a potential way to detect the enantiomeric excess of chiral mixture by monitoring the output field of the cavity.

## I. INTRODUCTION

Molecular chirality has attracted considerable interests due to its fundamental role in the enantio-selective biological activity, chemical reactions, and pharmaceutical processes [1–4]. The enantio-discrimination [5–18], spatial enantio-separation [19–25], and inner-state enantio-purification (including the enantio-specific state transfer [26–34] and enantio-conversion [35–42]) of chiral molecules are important and challenging tasks. Recently, the investigations have shown the great success in enantio-discrimination of chiral molecules via the enantiomer-specific microwave spectroscopic methods [43–48] based on the three-photon process in the cyclic three-level models [49–55] of chiral molecules. In these methods, when the chiral molecules are driven by two classical light fields, a new classical light field (whose frequency is the sum of or difference between those of the two existed ones) can be induced via the three-photon process of three-wave mixing [43–48]. Since the product of three Rabi frequencies for the cyclic three-level model can change sign with enantiomer, there is a phase shift of  $\pi$  between the new light fields generated from the left- and right- handed molecules. Thus, the difference between the numbers of left- and right- handed molecules is mapped on the total induced light field. Based on this, the enantiomeric excess of chiral mixture can be detected by monitoring the total induced light field.

In the past few years, the cavity-molecule(s) systems with a single molecule (many molecules) confined in the cavity [56–61] have attained much attention since the quantized cavity field is introduced to interact with the molecule(s). Recent investigations imply that there has been great progress in studying energy transfer [62, 63], control of chemical reactivity [64, 65], and molecular spectra [66, 67] based on such cavity-molecule(s) systems. Thus, the cavity-molecule(s) system may provide a new platform for the exploration in

enantio-discrimination of chiral molecules [61]. Note that the realistic systems for enantio-discrimination [5–18] (or spatial enantio-separation [19–25] and inner-state enantio-purification [26–42]) of chiral molecules usually involve a number of molecules. In the cases of many molecules coupled by only the classical light fields [5–18], the single-molecule treatment describing the interaction between single molecules and light fields is appropriate in studying the light-molecule interaction. However, when the quantized cavity field is introduced to couple with many molecules, the single-molecule treatment is usually no longer valid. Thus, it is required to introduce the multi-molecule treatment describing the collective interaction between many molecules and quantized cavity field [57, 59, 63, 64] to investigate the light-molecules interaction.

In this paper, we propose a theoretical method for the enantio-discrimination of chiral molecules via the cavity-assisted three-photon process in the cavity-molecules system with the multi-molecule treatment (instead of the single-molecule ones used in the previous enantiomer-specific microwave spectroscopic methods [43–48] of enantio-discrimination). Our system consists of a cavity without external driving and an ensemble of chiral mixture confined in the cavity. Each molecule is modeled as the cyclic three-level model coupled by the quantized cavity field and two classical light fields. Initially, the chiral molecules stay in their ground states, and the quantized cavity field is in the vacuum state. When the chiral molecules are driven by the two classical light fields, the intracavity photons can be generated continuously via the cavity-assisted three-photon process. Such a process is associated with the difference between the numbers of left- and right- handed molecules in the chiral mixture. Based on this, we can employ the multi-molecule treatment to investigate the cavity field as well as the output field of the cavity in the steady state and demonstrate the applications in the detection of the enantiomeric excess via measuring the intensity of the cavity output field.

This paper is organized as follows. In Sec. II, we present the Hamiltonian and quantum Langevin equations for the cavity-molecules system under consideration. Then the results for enantio-discrimination of chiral molecules in the case of low-

\* yechong@bit.edu.cn

† liyong@csrc.ac.cn

excitation limit of molecules are given in Sec. III via monitoring the cavity output field. In Sec. IV, we further focus on the case beyond low-excitation limit of molecules and present the results about the detection of the enantiomeric excess. Finally, we summarize the conclusion in section V.

## II. CAVITY-MOLECULES SYSTEM

We now consider the cavity-molecules system consisting of the cavity without external driving and the ensemble of  $N$  chiral molecules (confined in the cavity) as shown in Fig. 1. The ensemble contains  $N_L$  left-handed molecules and  $N_R$  right-handed molecules. Each molecule can be described by the cyclic three-level model, where the quantized cavity field with frequency  $\omega_a$  couples with the transition  $|2\rangle_Q \leftrightarrow |1\rangle_Q$  with transition frequency  $\omega_{21}$ . Meanwhile, the transition  $|3\rangle_Q \leftrightarrow |2\rangle_Q$  with transition frequency  $\omega_{32}$  is driven by the classical light field with frequency  $\nu_{32}$ , and the transition  $|3\rangle_Q \leftrightarrow |1\rangle_Q$  with transition frequency  $\omega_{31}$  is coupled by the classical light field with frequency  $\nu_{31}$ . Here, the intracavity photons are assumed to only leak out from the right side of the cavity for the sake of simplicity. The subscripts  $Q = L, R$  are introduced to denote the molecular chirality. We define the collective operator for the chiral molecules  $S_{jk}^Q = \sum_{m=1}^{N_Q} \sigma_{jk}^{Q(m)}$  with  $\sigma_{jk}^{Q(m)} = |j\rangle_{mm}^{QQ}\langle k|$  ( $j, k = 1, 2, 3$ ) denoting the transition operator for the  $m$ -th left- ( $Q = L$ ) or right-handed ( $Q = R$ ) molecule. Under the electric-dipole approximation and rotating-wave approximation, the Hamiltonian for the system is written as ( $\hbar = 1$ )

$$H = \omega_a a^\dagger a + \omega_{21}(S_{22}^L + S_{22}^R) + \omega_{31}(S_{33}^L + S_{33}^R) + [g_a a(S_{21}^L + S_{21}^R) + \Omega_{31} e^{-i\nu_{31}t}(S_{31}^L + S_{31}^R) + \Omega_{32} e^{-i\nu_{32}t}(e^{i\phi_L} S_{32}^L + e^{i\phi_R} S_{32}^R) + \text{H.c.}], \quad (1)$$

where  $a$  ( $a^\dagger$ ) represents the annihilation (creation) operator of the quantized cavity field.  $g_a = \mu_{21} \sqrt{\frac{\omega_a}{2\hbar\epsilon_0 V}}$  represents the coupling strength for single molecule to the quantized cavity field, with  $\mu_{21}$  being the electric-dipole transition moment of transition  $|2\rangle_Q \leftrightarrow |1\rangle_Q$ ,  $\epsilon_0$  denoting the permittivity of vacuum, and  $V$  being the mode volume of the cavity.  $\Omega_{31}$  and  $\Omega_{32}$  are the coupling strengths for the two classical light fields. These coupling strengths ( $g_a$ ,  $\Omega_{31}$ , and  $\Omega_{32}$ ) are taken to be identical

for all molecules by assuming the chiral mixture fixed in small volume whose size is much less than the typical wavelength. For simplicity but without loss of generality, these coupling strengths are taken as real. The chirality of the cyclic three-level model is specified by choosing the overall phases of left- and right-handed molecules as [12, 16, 19, 43]

$$\phi_L = \phi, \phi_R = \phi + \pi. \quad (2)$$

The Hamiltonian in the interaction picture with respect to  $H_0 = (\nu_{31} - \nu_{32})a^\dagger a + (\nu_{31} - \nu_{32})(S_{22}^L + S_{22}^R) + \nu_{31}(S_{33}^L + S_{33}^R)$  can be written in the time-independent form as

$$H_I = \Delta_a a^\dagger a + (\Delta_{31} - \Delta_{32})(S_{22}^L + S_{22}^R) + \Delta_{31}(S_{33}^L + S_{33}^R) + [g_a a(S_{21}^L + S_{21}^R) + \Omega_{31}(S_{31}^L + S_{31}^R) + \Omega_{32}(e^{i\phi_L} S_{32}^L + e^{i\phi_R} S_{32}^R) + \text{H.c.}], \quad (3)$$

where the detunings are  $\Delta_a = \omega_a + \nu_{32} - \nu_{31}$ ,  $\Delta_{31} = \omega_{31} - \nu_{31}$ , and  $\Delta_{32} = \omega_{32} - \nu_{32}$ .

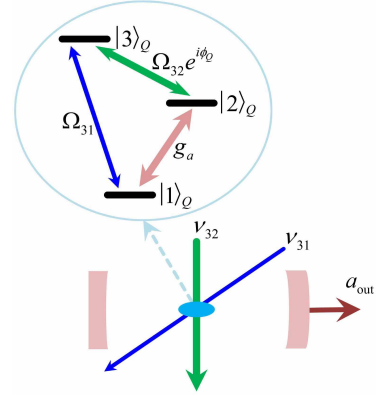


FIG. 1. The schematic diagram of the cavity-molecules system with the ensemble of  $N_L$  left-handed molecules and  $N_R$  right-handed molecules confined in the single-sided cavity. Each molecule is coupled with the quantized cavity field (with frequency  $\omega_a$ ) and two classical light fields (with frequencies  $\nu_{31}$  and  $\nu_{32}$ , respectively) to form the cyclic three-level model. The intracavity photons can only leak out from the right side of the cavity.

From the Hamiltonian (3), we can obtain the following quantum Langevin equations

$$\begin{aligned} \dot{a} &= -i\Delta_a a - i g_a (S_{12}^L + S_{12}^R) - \kappa_a a + \sqrt{2\kappa_a} a_{\text{in}}, \\ \dot{S}_{11}^Q &= i[g_a (a S_{21}^Q - a^\dagger S_{12}^Q) + \Omega_{31} (S_{31}^Q - S_{13}^Q)] + 2\Gamma_{21} S_{22}^Q + 2\Gamma_{31} S_{33}^Q + F_{11}^Q, \\ \dot{S}_{22}^Q &= i[g_a (a^\dagger S_{12}^Q - a S_{21}^Q) + \Omega_{32} (e^{i\phi_Q} S_{32}^Q - e^{-i\phi_Q} S_{23}^Q)] - 2\Gamma_{21} S_{22}^Q + 2\Gamma_{32} S_{33}^Q + F_{22}^Q, \\ \dot{S}_{12}^Q &= i[(\Delta_{32} - \Delta_{31}) S_{12}^Q + g_a a (S_{22}^Q - S_{11}^Q) + \Omega_{31} S_{32}^Q - \Omega_{32} e^{-i\phi_Q} S_{13}^Q] - \Gamma_{21} S_{12}^Q + F_{12}^Q, \\ \dot{S}_{13}^Q &= i[-\Delta_{31} S_{13}^Q + \Omega_{31} (S_{33}^Q - S_{11}^Q) + g_a a S_{23}^Q - \Omega_{32} e^{i\phi_Q} S_{12}^Q] - (\Gamma_{31} + \Gamma_{32}) S_{13}^Q + F_{13}^Q, \\ \dot{S}_{23}^Q &= i[-\Delta_{32} S_{23}^Q + \Omega_{32} e^{i\phi_Q} (S_{33}^Q - S_{22}^Q) - \Omega_{31} S_{21}^Q + g_a a^\dagger S_{13}^Q] - (\Gamma_{21} + \Gamma_{31} + \Gamma_{32}) S_{23}^Q + F_{23}^Q. \end{aligned} \quad (4)$$

Here,  $\kappa_a$  represents the decay rate from the right side of the cavity and we have neglected the other decay rate of the single-sided cavity.  $a_{\text{in}}$  denotes the quantum input noise operator of the cavity with zero-mean value (i.e.,  $\langle a_{\text{in}} \rangle = 0$ ).  $\Gamma_{21}$ ,

$\Gamma_{31}$ , and  $\Gamma_{32}$  are introduced to represent the decay rates of the molecules.  $F_{jk}^Q$  (with  $j, k = 1, 2, 3$ ) denotes the quantum noise term for the collective operator  $S_{jk}^Q$  with zero-mean value (i.e.,  $\langle F_{jk}^Q \rangle = 0$ ). Taking the mean-field approximation [68], we can obtain the corresponding steady-state equations as

$$\begin{aligned}
0 &= -(i\Delta_a + \kappa_a)\langle a \rangle - ig_a(\langle S_{12}^L \rangle + \langle S_{12}^R \rangle), \\
0 &= ig_a(\langle a \rangle \langle S_{21}^Q \rangle - \langle a^\dagger \rangle \langle S_{12}^Q \rangle) + i\Omega_{31}(\langle S_{31}^Q \rangle - \langle S_{13}^Q \rangle) + 2\Gamma_{21}\langle S_{22}^Q \rangle + 2\Gamma_{31}\langle S_{33}^Q \rangle, \\
0 &= ig_a(\langle a^\dagger \rangle \langle S_{12}^Q \rangle - \langle a \rangle \langle S_{21}^Q \rangle) + i\Omega_{32}(e^{i\phi_Q}\langle S_{32}^Q \rangle - e^{-i\phi_Q}\langle S_{23}^Q \rangle) - 2\Gamma_{21}\langle S_{22}^Q \rangle + 2\Gamma_{32}\langle S_{33}^Q \rangle, \\
0 &= -[i(\Delta_{31} - \Delta_{32}) + \Gamma_{21}]\langle S_{12}^Q \rangle + ig_a\langle a \rangle(\langle S_{22}^Q \rangle - \langle S_{11}^Q \rangle) + i\Omega_{31}\langle S_{32}^Q \rangle - i\Omega_{32}e^{-i\phi_Q}\langle S_{13}^Q \rangle, \\
0 &= -[i\Delta_{31} + (\Gamma_{31} + \Gamma_{32})]\langle S_{13}^Q \rangle + i\Omega_{31}(\langle S_{33}^Q \rangle - \langle S_{11}^Q \rangle) + ig_a\langle a \rangle \langle S_{23}^Q \rangle - i\Omega_{32}e^{i\phi_Q}\langle S_{12}^Q \rangle, \\
0 &= -[i\Delta_{32} + (\Gamma_{21} + \Gamma_{31} + \Gamma_{32})]\langle S_{23}^Q \rangle + i\Omega_{32}e^{i\phi_Q}(\langle S_{33}^Q \rangle - \langle S_{22}^Q \rangle) - i\Omega_{31}\langle S_{21}^Q \rangle + ig_a\langle a^\dagger \rangle \langle S_{13}^Q \rangle,
\end{aligned} \tag{5}$$

where  $\langle O \rangle$  (with  $O = a, a^\dagger, S_{jk}^Q$ ) denotes the mean value of the operator. Moreover, the collective operators  $\langle S_{jj}^Q \rangle$  (with  $j = 1, 2, 3$ ) satisfy the relation  $\sum_{j=1}^3 \langle S_{jj}^Q \rangle = N_Q$ .

### III. ENANTIO-DISCRIMINATION: LOW-EXCITATION LIMIT OF MOLECULES

In this section, we investigate the steady-state output field of the cavity in the case of low-excitation limit of molecules and explore its potential applications in the detection of enantio-discrimination. Here, we consider the case of weak coupling strength  $\Omega_{31} \ll \Gamma_{31}$  since such a weak coupling strength can usually ensure the low-excitation limit of molecules where most molecules stay in their ground states in our system. At the end of this section, we will verify the validity of such a limit for the parameters being used.

#### A. Steady-state intensity of the output field

For the case of weak coupling strength  $\Omega_{31} \ll \Gamma_{31}$ , one can treat  $\Omega_{31}$  as a perturbation. Hence, we apply the perturbation approach to the element  $\langle O \rangle$ , which is given in terms of perturbation expansion [69] with respect to  $\Omega_{31}$  as

$$\langle O \rangle = \langle O \rangle^{(0)} + \langle O \rangle^{(1)} + \langle O \rangle^{(2)} + \dots, \tag{6}$$

where  $\langle O \rangle^{(n)}$  ( $n = 0, 1, \dots$ ) is the  $n$ -th-order solution of  $\langle O \rangle$ . The zeroth-order solution  $\langle O \rangle^{(0)}$  describes the case in the absence of the classical light field  $\Omega_{31}$ . In such a case, no photon is generated, and thus the molecules in the initial ground state  $|1\rangle_Q$  cannot be stimulated to the excited states  $|2\rangle_Q$  and  $|3\rangle_Q$ . Therefore, the zeroth-order solutions are given by

$$\begin{aligned}
\langle a \rangle^{(0)} &= 0, \quad \langle S_{11}^Q \rangle^{(0)} = N_Q, \\
\langle S_{22}^Q \rangle^{(0)} &= \langle S_{33}^Q \rangle^{(0)} = 0, \quad \langle S_{jk}^Q \rangle^{(0)} = 0 \quad (k \neq j).
\end{aligned} \tag{7}$$

Substituting Eq. (6) into Eq. (5) and treating  $\Omega_{31}$  as a perturbation, one can find that the first-order solutions satisfy the following equations

$$\begin{aligned}
0 &= -(i\Delta_a + \kappa_a)\langle a \rangle^{(1)} - ig_a[\langle S_{12}^L \rangle^{(1)} + \langle S_{12}^R \rangle^{(1)}], \\
0 &= ig_a[\langle a \rangle^{(1)} \langle S_{21}^Q \rangle^{(0)} + \langle a \rangle^{(0)} \langle S_{21}^Q \rangle^{(1)} - \langle a^\dagger \rangle^{(1)} \langle S_{12}^Q \rangle^{(0)} - \langle a^\dagger \rangle^{(0)} \langle S_{12}^Q \rangle^{(1)}] + i\Omega_{31}[\langle S_{31}^Q \rangle^{(0)} - \langle S_{13}^Q \rangle^{(0)}] + 2\Gamma_{21}\langle S_{22}^Q \rangle^{(1)} + 2\Gamma_{31}\langle S_{33}^Q \rangle^{(1)}, \\
0 &= ig_a[\langle a^\dagger \rangle^{(1)} \langle S_{12}^Q \rangle^{(0)} + \langle a^\dagger \rangle^{(0)} \langle S_{12}^Q \rangle^{(1)} - \langle a \rangle^{(1)} \langle S_{21}^Q \rangle^{(0)} - \langle a \rangle^{(0)} \langle S_{21}^Q \rangle^{(1)}] + i\Omega_{32}[e^{i\phi_Q}\langle S_{32}^Q \rangle^{(1)} - e^{-i\phi_Q}\langle S_{23}^Q \rangle^{(1)}] \\
&\quad - 2\Gamma_{21}\langle S_{22}^Q \rangle^{(1)} + 2\Gamma_{32}\langle S_{33}^Q \rangle^{(1)}, \\
0 &= -[i(\Delta_{31} - \Delta_{32}) + \Gamma_{21}]\langle S_{12}^Q \rangle^{(1)} + ig_a\langle a \rangle^{(1)}[\langle S_{22}^Q \rangle^{(0)} - \langle S_{11}^Q \rangle^{(0)}] + ig_a\langle a \rangle^{(0)}[\langle S_{22}^Q \rangle^{(1)} - \langle S_{11}^Q \rangle^{(1)}] \\
&\quad + i\Omega_{31}\langle S_{32}^Q \rangle^{(0)} - i\Omega_{32}e^{-i\phi_Q}\langle S_{13}^Q \rangle^{(1)}, \\
0 &= -[i\Delta_{31} + (\Gamma_{31} + \Gamma_{32})]\langle S_{13}^Q \rangle^{(1)} + i\Omega_{31}[\langle S_{33}^Q \rangle^{(0)} - \langle S_{11}^Q \rangle^{(0)}] + ig_a\langle a \rangle^{(1)}\langle S_{23}^Q \rangle^{(0)} + ig_a\langle a \rangle^{(0)}\langle S_{23}^Q \rangle^{(1)} - i\Omega_{32}e^{i\phi_Q}\langle S_{12}^Q \rangle^{(1)}, \\
0 &= -[i\Delta_{32} + (\Gamma_{21} + \Gamma_{31} + \Gamma_{32})]\langle S_{23}^Q \rangle^{(1)} + i\Omega_{32}e^{i\phi_Q}[\langle S_{33}^Q \rangle^{(1)} - \langle S_{22}^Q \rangle^{(1)}] - i\Omega_{31}\langle S_{21}^Q \rangle^{(0)} + ig_a\langle a^\dagger \rangle^{(1)}\langle S_{13}^Q \rangle^{(0)} + ig_a\langle a^\dagger \rangle^{(0)}\langle S_{13}^Q \rangle^{(1)}, \\
0 &= \langle S_{11}^Q \rangle^{(1)} + \langle S_{22}^Q \rangle^{(1)} + \langle S_{33}^Q \rangle^{(1)}.
\end{aligned} \tag{8}$$

From Eqs. (2) and (8), we can get the first-order solution of  $\langle a \rangle$  as

$$\langle a \rangle^{(1)} = \frac{i(N_L - N_R)g_a\Omega_{31}\Omega_{32}e^{-i\phi}}{K_a(K_{21}K_{31} + \Omega_{32}^2) + g_a^2NK_{31}}, \quad (9)$$

where  $K_a = i\Delta_a + \kappa_a$ ,  $K_{21} = i(\Delta_{31} - \Delta_{32}) + \Gamma_{21}$ , and  $K_{31} = i\Delta_{31} + \Gamma_{31} + \Gamma_{32}$ . For the case of weak coupling strength  $\Omega_{31}$ , the first-order solution  $\langle a \rangle^{(1)}$  can sufficiently reflect the main physical properties of  $\langle a \rangle$ . Therefore, we here take the approximation  $\langle a \rangle \simeq \langle a \rangle^{(1)}$ .

In our system, the intracavity photons are assumed to only leak out from the right side of the cavity. Using the input-output relation of the single-sided cavity without external driving [70, 71]

$$\sqrt{2\kappa_a}a = a_{\text{in}} + a_{\text{out}}, \quad (10)$$

we can obtain the mean output field from the right side of the cavity  $\langle a_{\text{out}} \rangle = \sqrt{2\kappa_a}\langle a \rangle$ . It is found that such a mean output field depends on the difference between the numbers of left- and right-handed molecules (i.e.,  $N_L - N_R$ ). This can be understood as follows. When the ensemble of chiral mixture confined in the cavity is driven by the two classical light fields, the cavity-assisted three-photon process [see from the term  $g_a\Omega_{31}\Omega_{32}$  in the numerator of Eq. (9)] can lead to the continuous generation of intracavity photons. Since  $g_a\Omega_{31}\Omega_{32}e^{i\phi_Q}$  can change sign with enantiomer, the total contributions of the cavity-assisted three-photon processes for the left- and right-handed molecules to the output field of cavity is dependent on  $N_L - N_R$ . This will give rise to the mean output field determined by  $N_L - N_R$ .

According to the definition  $I_{\text{out}} = |\langle a_{\text{out}} \rangle|^2$ , one can further obtain the intensity of the output field as

$$I_{\text{out}} = \left| \frac{N\sqrt{2\kappa_a}g_a\Omega_{31}\Omega_{32}\eta}{K_a(K_{21}K_{31} + \Omega_{32}^2) + g_a^2NK_{31}} \right|^2, \quad (11)$$

where  $\eta = \frac{N_L - N_R}{N_L + N_R}$  denotes the enantiomeric excess. From Eq. (11), it is found that the intensity of the output field  $I_{\text{out}}$  does not depend on the overall phase  $\phi$ .

## B. Detection of the enantiomeric excess

So far, we have obtained the intensity of the output field  $I_{\text{out}}$  via the cavity-assisted three-photon process. In the following analysis and simulations in this section, we will focus on the strong collective coupling condition [72–75]  $g_a\sqrt{N} \gg \{\Gamma_{21}, \Gamma_{31}, \Gamma_{32}, \Omega_{32}, \Omega_{31}, \kappa_a\}$ . Meanwhile, we take  $\Delta_{31} = 0$  (i.e., the transition  $|3\rangle_Q \leftrightarrow |1\rangle_Q$  is resonantly coupled by the classical light field  $\Omega_{31}$ ) and  $\omega_a = \omega_{21}$  (i.e., the transition  $|2\rangle_Q \leftrightarrow |1\rangle_Q$  is resonantly coupled with the quantized cavity field), which means  $\Delta_a \equiv -\Delta_{32}$ .

In Fig. 2, we give the intensity of the output field  $I_{\text{out}}$  versus the detuning  $\Delta_{32}$  for different enantiomeric excess  $\eta$ . Here, we assume the total number of chiral molecules  $N = 10^6$  [59, 63, 64, 67] and weak coupling strength  $\Omega_{31} = 0.05\Gamma_{31}$ . It is

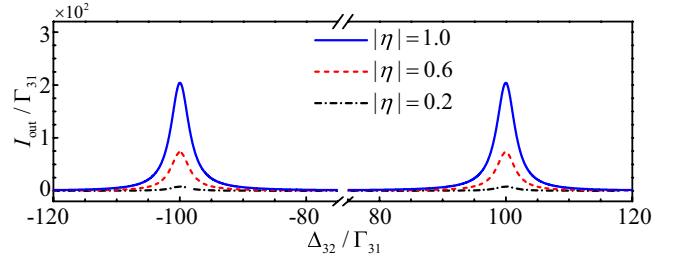


FIG. 2. The intensity of the output field as a function of the detuning  $\Delta_{32}$  for different enantiomeric excess  $\eta$ . The other parameters are chosen as  $\Gamma_{21} = \Gamma_{32} = \Gamma_{31}$ ,  $\kappa_a = 2\Gamma_{31}$ ,  $\Delta_{31} = 0$ ,  $\Delta_a = -\Delta_{32}$ ,  $\Omega_{31} = 0.05\Gamma_{31}$ ,  $\Omega_{32} = \Gamma_{31}$ ,  $g_a = 0.1\Gamma_{31}$ , and  $N = 10^6$ .

shown that there exist two characteristic peaks at the detuning  $\Delta_{32} \simeq \pm g_a\sqrt{N}$ . This can be understood as the result of the quantized cavity field in the strong collective coupling condition [63, 64, 68, 76–79]. At the positions of the two characteristic peaks  $\Delta_{32} \simeq \pm g_a\sqrt{N}$ ,  $I_{\text{out}}$  is relatively sensitive to  $\eta$  compared with those at other detunings. Thus, we here focus on the cavity output intensity  $I_{\text{out}}^{\text{max}}$  at  $\Delta_{32} = g_a\sqrt{N}$ , which can be obtained as

$$I_{\text{out}}^{\text{max}} \simeq \frac{2N\kappa_a\Omega_{31}^2\Omega_{32}^2\eta^2}{[(\Gamma_{31} + \Gamma_{32})(\Gamma_{21} + \kappa_a) + \Omega_{32}^2]^2} \quad (12)$$

by substituting  $\Delta_{32} = g_a\sqrt{N}$  into Eq. (11) and taking the approximation  $g_a\sqrt{N} \gg \{\Gamma_{21}, \Gamma_{31}, \Gamma_{32}, \Omega_{32}, \Omega_{31}, \kappa_a\}$ .

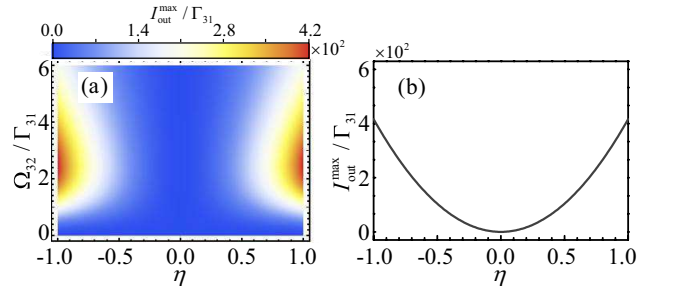


FIG. 3. (a) The cavity output intensity  $I_{\text{out}}^{\text{max}}$  versus the enantiomeric excess  $\eta$  and coupling strength  $\Omega_{32}$ . (b) The cavity output intensity  $I_{\text{out}}^{\text{max}}$  versus the enantiomeric excess  $\eta$  for  $\Omega_{32} = 2.5\Gamma_{31}$ . The other parameters are the same as those in Fig. 2 except for  $\Delta_{32} = g_a\sqrt{N}$ .

Moreover, the cavity output intensity  $I_{\text{out}}^{\text{max}}$  versus the enantiomeric excess  $\eta$  and coupling strength  $\Omega_{32}$  is displayed in Fig. 3(a). One can find that  $I_{\text{out}}^{\text{max}}$  strongly depends on the coupling strength  $\Omega_{32}$ . When  $\Omega_{32} \simeq 2.5\Gamma_{31}$ , the cavity output intensity for  $|\eta| = 1$  can reach the maximum  $I_{\text{out}}^{\text{max}} \simeq 420\Gamma_{31}$  [see Fig. 3(b)].

We would like to remark that the above discussions are based on the low-excitation limit of molecules in the case of weak coupling strength  $\Omega_{31}$ . Thus, we should verify whether they can meet the requirement for such a limit. Here, the factor

$$P_e^Q = \frac{\langle S_{22}^Q \rangle + \langle S_{33}^Q \rangle}{N_Q} \quad (13)$$

is introduced to describe the proportion of the left- (right-) handed molecules occupying the excited states  $|2\rangle_L$  and  $|3\rangle_L$  ( $|2\rangle_R$  and  $|3\rangle_R$ ) to the total left- (right-) handed molecules. The steady-state values  $\langle S_{22}^O \rangle$  and  $\langle S_{33}^O \rangle$  can be obtained by numerically solving Eq. (5). For the parameters in Figs. 2 and 3, we find that the factor is  $P_e^O < 0.3\%$ . This implies that most of the molecules occupy the ground states and thus the results meet the requirement for the low-excitation limit of molecules in the above discussions.

#### IV. ENANTIO-DISCRIMINATION: BEYOND LOW-EXCITATION LIMIT OF MOLECULES

In the last section, we have investigated the steady-state output field of the cavity in the case of low-excitation limit of molecules. The results show that the enantiomeric excess can be detected by measuring the intensity of the output field. In this section, we further study the steady-state output field of the cavity in the case beyond low-excitation limit of molecules.

##### A. Steady-state intensity of the output field

When considering the case beyond low-excitation limit of molecules, one can obtain the steady-state value  $\langle a \rangle$  by numerically solving the steady-state equations (5). Using the input-output relation (10), we can also obtain the mean output field  $\langle a_{\text{out}} \rangle = \sqrt{2\kappa_a} \langle a \rangle$  and its intensity  $I_{\text{out}} = |\langle a_{\text{out}} \rangle|^2$ .

##### B. Detection of the enantiomeric excess

In the following analysis and simulations in this section, the decay rates ( $\kappa_a$ ,  $\Gamma_{21}$ ,  $\Gamma_{31}$ , and  $\Gamma_{32}$ ), detunings ( $\Delta_a$  and  $\Delta_{31}$ ), coupling strength  $g_a$ , and total numbers of chiral molecules  $N$  are taken as the same values as those in the case of low-excitation limit of molecules. Meanwhile, we choose the coupling strength  $\Omega_{32} = 2.5\Gamma_{31}$  and overall phase  $\phi = 0$ .

Since the enhancement of  $\Omega_{31}$  can lead to the molecules occupying their excited states, we here take the coupling strength  $\Omega_{31} = 0.2\Gamma_{31}$  larger than that considered in the case of low-excitation limit of molecules. Similar as the case of low-excitation limit of molecules, there are two characteristic peaks for  $I_{\text{out}}$  [see Fig. 4(a)]. Differently, the positions of the characteristic peaks here can vary slightly with  $\eta$  near the detuning  $\Delta_{32} \simeq \pm g_a \sqrt{N}$ . For simplicity, we still focus on the cavity output intensity  $I_{\text{out}}^{\text{max}}$  at  $\Delta_{32} = g_a \sqrt{N}$  in the detection of enantiomeric excess. Note that the cavity output intensity  $I_{\text{out}}^{\text{max}}$  is enhanced dramatically [e.g.,  $I_{\text{out}}^{\text{max}} \geq 6000\Gamma_{31}$  for  $\eta = -1$  as shown in Fig. 4(b)]. That means much more photons are generated via the cavity-assisted three-photon process compared with the case of low-excitation limit of molecules. Therefore, the cavity output intensity  $I_{\text{out}}^{\text{max}}$  here may provide the promising applications in high performance detection of enantiomeric excess. Meanwhile,  $I_{\text{out}}^{\text{max}}$  is different for the enantiopure left- ( $\eta = 1$ ) and right- ( $\eta = -1$ ) handed molecules.

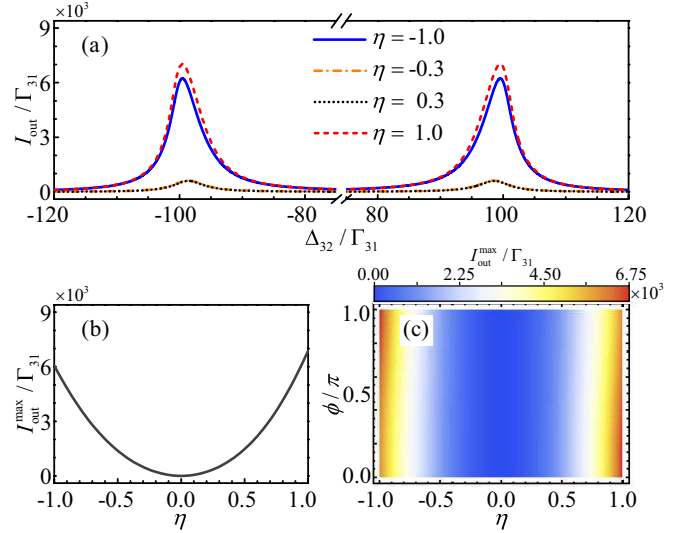


FIG. 4. (a) The intensity of the output field  $I_{\text{out}}$  as a function of the detuning  $\Delta_{32}$  for different enantiomeric excess  $\eta$ . (b) The cavity output intensity  $I_{\text{out}}^{\text{max}}$  versus the enantiomeric excess  $\eta$ . (c) The cavity output intensity  $I_{\text{out}}^{\text{max}}$  versus the enantiomeric excess  $\eta$  and overall phase  $\phi$ . The other parameters are the same as those in Fig. 2 except for  $\Delta_{32} = g_a \sqrt{N}$ ,  $\Omega_{31} = 0.2\Gamma_{31}$ ,  $\Omega_{32} = 2.5\Gamma_{31}$ , and  $\phi = 0$ .

Additionally, one can find that the cavity output intensity  $I_{\text{out}}^{\text{max}}$  also depends on the overall phase  $\phi$  [see Fig. 4(c)]. This is different from the case of low-excitation limit of molecules where  $I_{\text{out}}^{\text{max}}$  does not depend on  $\phi$ . When taking  $\phi \sim 0 - 0.1\pi$ ,  $I_{\text{out}}^{\text{max}}$  can be relatively sensitive to the enantiomeric excess  $\eta$  compared with those for other  $\phi$ . Hence, for simplicity, we assume the overall phase  $\phi = 0$  in the following discussions.

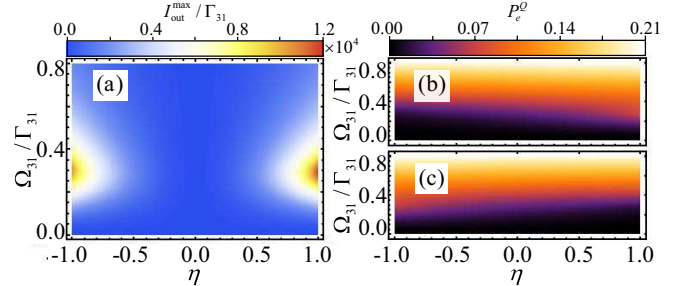


FIG. 5. (a) The cavity output intensity  $I_{\text{out}}^{\text{max}}$ , (b) the factor  $P_e^L$ , and (c) the factor  $P_e^R$  versus the enantiomeric excess  $\eta$  and coupling strength  $\Omega_{31}$ . The other parameters are the same as those in Fig. 4.

Further, we give the cavity output intensity  $I_{\text{out}}^{\text{max}}$  versus the enantiomeric excess  $\eta$  and coupling strength  $\Omega_{31}$  in Fig. 5(a). It is shown that  $I_{\text{out}}^{\text{max}}$  strongly depends on the coupling strength  $\Omega_{31}$ . For the coupling strength  $\Omega_{31} \sim 0.25 - 0.35\Gamma_{31}$ , a certain proportion of the molecules occupies the excited states [see Figs. 5(b) and 5(c)], and the cavity-assisted three-photon process enables the continuous generation of more intracavity photons compared with the case of weak coupling strength (e.g.,  $\Omega_{31} = 0.05\Gamma_{31}$ ). This can lead to the dramatical enhancement of the cavity output intensity. Therefore, by ad-

justing the coupling strength  $\Omega_{31}$  appropriately,  $I_{\text{out}}^{\text{max}}$  can be enhanced further, which can improve the resolution in the detection of the enantiomeric excess via measuring the cavity output intensity.

## V. CONCLUSION

In conclusion, we have proposed a theoretical method for the enantio-discrimination of chiral molecules via the cavity-assisted three-photon process in the cavity-molecules system. The key idea is to generate the intracavity photons via the cavity-assisted three-photon process based on the cyclic three-level models of chiral molecules. In the low-excitation limit of molecules, our analytic results show the steady-state output intensity of the cavity is proportional to the square of the enantiomeric excess, which provides the method for enantio-discrimination of chiral molecules by monitoring the cavity output field. Furthermore, beyond the low-excitation limit of molecules, we present the results for enantio-discrimination based on the numerical solution of the cavity output intensity. It is found that with increasing the coupling strength (e.g.,  $\Omega_{31} = 0.3\Gamma_{31}$ ), more intracavity photons are generated compared with the case of weak coupling strength (e.g.,

$\Omega_{31} = 0.05\Gamma_{31}$ ). Thus, the cavity output intensity in the case beyond low-excitation limit of molecules can be enhanced dramatically. This offers the possibility of high performance detection of enantiomeric excess via measuring the cavity output intensity.

We would like to remark that in the previous enantiomer-specific microwave spectroscopic methods for enantio-discrimination of chiral molecules [43–48], the single-molecule treatment was usually used due to the fact that only the classical optical fields are involved. However, in our cavity-molecules system, the chiral molecules confined in the cavity are collectively coupled to the quantized cavity field. Therefore, we should resort to the multi-molecule treatment [57, 59, 63, 64] since the single-molecule one is no longer valid in the present cavity-molecules system.

## ACKNOWLEDGMENTS

This work was supported by the Natural Science Foundation of China (Grants No. 12074030, No. 11947206, No. 11774024, and No. U1930402), the National Key R&D Program of China (Grant No. 2016YFA0301200), and the Science Challenge Project (Grant No. TZ2018003).

- 
- [1] N. P. Franks and W. R. Lieb, “Stereospecific Effects of Inhalational General Anesthetic Optical Isomers on Nerve Ion Channels,” *Science* **254**, 427 (1991).
- [2] A. J. Hutt and S. C. Tan, “Drug Chirality and its Clinical Significance,” *Drugs* **52**, 1 (1996).
- [3] K. Bodenhofer, A. Hierlemann, J. Seemann, G. Gauglitz, B. Koppenhofer, and W. Gopel, “Chiral Discrimination Using Piezoelectric and Optical Gas Sensors,” *Nature (London)* **387**, 577 (1997).
- [4] J. Gal, “The Discovery of Stereoselectivity at Biological Receptors: Arnaldo Piutti and the Taste of the Asparagine Enantiomers—History and Analysis on the 125th Anniversary,” *Chirality* **12**, 959 (2012).
- [5] L. D. Barron, *Molecular Light Scattering and Optical Activity* (Cambridge University Press, Cambridge, UK, 1982).
- [6] E. A. Power and T. Thirunamachandran, “Maxwell Fields Near a Chiral Molecule: Application to Induced Circular Dichroism,” *Proc. R. Soc. Lond. A* **396**, 155 (1984).
- [7] P. J. Stephens, “Theory of Vibrational Circular Dichroism,” *J. Phys. Chem.* **89**, 748 (1985).
- [8] R. K. Kondru, Peter Wipf, and D. N. Beratan, “Atomic contributions to the optical rotation angle as a quantitative probe of molecular chirality,” *Science* **282**, 2247 (1998).
- [9] G. L. J. A. Rikken and E. Raupach, “Enantioselective magnetochiral photochemistry,” *Nature (London)* **405**, 932 (2000).
- [10] H. Zepik, E. Shavit, M. Tang, T. R. Jensen, K. Kjaer, G. Bolbach, L. Leiserowitz, I. Weissbuch, and M. Lahav, “Chiral Amplification of Oligopeptides in Two-Dimensional Crystalline Self-Assemblies on Water,” *Science* **295**, 1266 (2002).
- [11] R. Bielski and M. Tencer, “Absolute enantioselective separation: Optical activity ex machina,” *J. Sep. Sci.* **28**, 2325 (2005).
- [12] W. Z. Jia and L. F. Wei, “Probing molecular chirality by coherent optical absorption spectra,” *Phys. Rev. A* **84**, 053849 (2011).
- [13] T. Wu, J. Ren, R. Wang, and X. Zhang, “Competition of Chiroptical Effect Caused by Nanostructure and Chiral Molecules,” *J. Phys. Chem. C* **118**, 20529 (2014).
- [14] D. Zhai, P. Wang, R.-Y. Wang, X. Tian, Y. Ji, W. Zhao, L. Wang, H. Wei, X. Wu, and X. Zhang, “Plasmonic polymers with strong chiroptical response for sensing molecular chirality,” *Nanoscale* **7**, 10690 (2015).
- [15] K. K. Lehmann, “Influence of spatial degeneracy on rotational spectroscopy: Three-wave mixing and enantiomeric state separation of chiral molecules,” *J. Chem. Phys.* **149**, 094201 (2018).
- [16] C. Ye, Q. Zhang, Y.-Y. Chen, and Y. Li, “Determination of enantiomeric excess with chirality-dependent ac Stark effects in cyclic three-level models,” *Phys. Rev. A* **100**, 033411 (2019).
- [17] X.-W. Xu, C. Ye, Y. Li, and A.-X. Chen, “Enantiomeric-excess determination based on nonreciprocal-transition-induced spectral-line elimination,” *Phys. Rev. A* **102**, 033727 (2020).
- [18] Y.-Y. Chen, C. Ye, Q. Zhang, and Y. Li, “Enantio-discrimination via light deflection effect,” *J. Chem. Phys.* **152**, 204305 (2020).
- [19] Y. Li, C. Bruder, and C. P. Sun, “Generalized Stern-Gerlach Effect for Chiral Molecules,” *Phys. Rev. Lett.* **99**, 130403 (2007).
- [20] X. Li and M. Shapiro, “Theory of the optical spatial separation of racemic mixtures of chiral molecules,” *J. Chem. Phys.* **132**, 194315 (2010).
- [21] A. Jacob and K. Hornberger, “Effect of molecular rotation on enantioseparation,” *J. Chem. Phys.* **137**, 044313 (2012).
- [22] A. Eilam and M. Shapiro, “Spatial Separation of Dimers of Chiral Molecules,” *Phys. Rev. Lett.* **110**, 213004 (2013).
- [23] R. P. Cameron, S. M. Barnett, and A. M. Yao, “Discriminatory optical force for chiral molecules,” *New J. Phys.* **16**, 013020 (2014).
- [24] D. S. Bradshaw and D. L. Andrews, “Chiral discrimination in optical trapping and manipulation,” *New J. Phys.* **16**, 103021 (2014).

- (2014).
- [25] P. Barcellona, R. Passante, L. Rizzuto, and S. Y. Buhmann, "Dynamical Casimir-Polder interaction between a chiral molecule and a surface," *Phys. Rev. A* **93**, 032508 (2016).
- [26] Y. Li and C. Bruder, "Dynamic method to distinguish between left- and right-handed chiral molecules," *Phys. Rev. A* **77**, 015403 (2008).
- [27] W. Z. Jia and L. F. Wei, "Distinguishing left- and right-handed molecules using two-step coherent pulses," *J. Phys. B: At. Mol. Opt. Phys.* **43**, 185402 (2010).
- [28] S. Eibenberger, J. M. Doyle, and D. Patterson, "Enantiomer-Specific State Transfer of Chiral Molecules," *Phys. Rev. Lett.* **118**, 123002 (2017).
- [29] C. Pérez, A. L. Steber, S. R. Domingos, A. Krin, D. Schmitz, and M. Schnell, "Coherent Enantiomer-Selective Population Enrichment Using Tailored Microwave Fields," *Angew. Chem. Int. Ed.* **56**, 12512 (2017).
- [30] C. Ye, Q. Zhang, Y.-Y. Chen, and Y. Li, "Effective two-level models for highly efficient inner-state enantioseparation based on cyclic three-level systems of chiral molecules," *Phys. Rev. A* **100**, 043403 (2019).
- [31] M. Leibscher, T. F. Giesen, and C. P. Koch, "Principles of enantio-selective excitation in three-wave mixing spectroscopy of chiral molecules," *J. Chem. Phys.* **151**, 014302 (2019).
- [32] Q. Zhang, Y.-Y. Chen, C. Ye, and Y. Li, "Evading thermal population influence on enantiomer-specific state transfer based on a cyclic three-level system via ro-vibrational transitions," *J. Phys. B: At. Mol. Opt. Phys.* **53**, 235103 (2020).
- [33] B. T. Torosov, M. Drewsen, and N. V. Vitanov, "Efficient and robust chiral resolution by composite pulses," *Phys. Rev. A* **101**, 063401 (2020).
- [34] B. T. Torosov, M. Drewsen, and N. V. Vitanov, "Chiral resolution by composite Raman pulses," *Phys. Rev. Research* **2**, 043235 (2020).
- [35] M. Shapiro, E. Frishman, and P. Brumer, "Coherently Controlled Asymmetric Synthesis with Achiral Light," *Phys. Rev. Lett.* **84**, 1669 (2000).
- [36] D. Gerbasi, M. Shapiro, and P. Brumer, "Theory of enantiomeric control in dimethylallene using achiral light," *J. Chem. Phys.* **115**, 5349 (2001).
- [37] P. Brumer, E. Frishman, and M. Shapiro, "Principles of electric-dipole-allowed optical control of molecular chirality," *Phys. Rev. A* **65**, 015401 (2001).
- [38] P. Král, I. Thannopulos, M. Shapiro, and D. Cohen, "Two-Step Enantio-Selective Optical Switch," *Phys. Rev. Lett.* **90**, 033001 (2003).
- [39] E. Frishman, M. Shapiro, and P. Brumer, "Optical purification of racemic mixtures by 'laser distillation' in the presence of a dissipative bath," *J. Phys. B: At. Mol. Opt. Phys.* **37**, 2811 (2004).
- [40] C. Ye, Q. Zhang, Y.-Y. Chen, and Y. Li, "Fast enantioconversion of chiral mixtures based on a four-level double- $\Delta$  model," *Phys. Rev. Research* **2**, 033064 (2020).
- [41] C. Ye, Q. Zhang, Y.-Y. Chen, and Y. Li, arXiv: 2001.07834 (2020).
- [42] C. Ye, B. Liu, Y.-Y. Chen, and Y. Li, arXiv: 2008.09810 (2020).
- [43] D. Patterson, M. Schnell, and J. M. Doyle, "Enantiomer-specific detection of chiral molecules via microwave spectroscopy," *Nature (London)* **497**, 475 (2013).
- [44] D. Patterson and J. M. Doyle, "Sensitive Chiral Analysis via Microwave Three-Wave Mixing," *Phys. Rev. Lett.* **111**, 023008 (2013).
- [45] D. Patterson and M. Schnell, "New studies on molecular chirality in the gas phase: enantiomer differentiation and determination of enantiomeric excess," *Phys. Chem. Chem. Phys.* **16**, 11114 (2014).
- [46] V. A. Shubert, D. Schmitz, D. Patterson, J. M. Doyle, and M. Schnell, "Identifying Enantiomers in Mixtures of Chiral Molecules with Broadband Microwave Spectroscopy," *Angew. Chem. Int. Ed.* **53**, 1152 (2014).
- [47] S. Lobsiger, C. Pérez, L. Evangelisti, K. K. Lehmann, and B. H. Pate, "Molecular Structure and Chirality Detection by Fourier Transform Microwave Spectroscopy," *J. Phys. Chem. Lett.* **6**, 196 (2015).
- [48] V. A. Shubert, D. Schmitz, C. Pérez, C. Medcraft, A. Krin, S. R. Domingos, D. Patterson, and M. Schnell, "Chiral Analysis Using Broadband Rotational Spectroscopy," *J. Phys. Chem. Lett.* **7**, 341 (2015).
- [49] P. Král and M. Shapiro, "Cyclic Population Transfer in Quantum Systems with Broken Symmetry," *Phys. Rev. Lett.* **87**, 183002 (2001).
- [50] Y. Liu, J. Q. You, L. F. Wei, C. P. Sun, and F. Nori, "Optical Selection Rules and Phase-Dependent Adiabatic State Control in a Superconducting Quantum Circuit," *Phys. Rev. Lett.* **95**, 087001 (2005).
- [51] E. Hirota, "Triple resonance for a three-level system of a chiral molecule," *Proc. Jpn. Acad. Ser. B* **88**, 120 (2012).
- [52] C. Ye, Q. Zhang, and Y. Li, "Real single-loop cyclic three-level configuration of chiral molecules," *Phys. Rev. A* **98**, 063401 (2018).
- [53] N. V. Vitanov and M. Drewsen, "Highly Efficient Detection and Separation of Chiral Molecules through Shortcuts to Adiabaticity," *Phys. Rev. Lett.* **122**, 173202 (2019).
- [54] J.-L. Wu, Y. Wang, J.-X. Han, C. Wang, S.-L. Su, Y. Xia, Y.-Y. Jiang, and J. Song, "Two-Path Interference for Enantiomer-Selective State Transfer of Chiral Molecules," *Phys. Rev. Applied* **13**, 044021 (2020).
- [55] J.-L. Wu, Y. Wang, S.-L. Su, Y. Xia, Y. Jiang, and J. Song, "Discrimination of enantiomers through quantum interference and quantum Zeno effect," *Opt. Express* **28**, 33475 (2020).
- [56] J. Flicka, M. Ruggenthaler, H. Appela, and A. Rubio, "Atoms and molecules in cavities, from weak to strong coupling in quantum-electrodynamics (QED) chemistry," *Proc. Natl. Acad. Sci.* **114**, 3026 (2017).
- [57] M. Reitz, C. Sommer, and C. Genes, "Langevin Approach to Quantum Optics with Molecules," *Phys. Rev. Lett.* **122**, 203602 (2019).
- [58] D. Wang, H. Kelkar, D. Martin-Cano, D. Rattenbacher, A. Shkarin, T. Utikal, S. Götzinger, and V. Sandoghdar, "Turning a molecule into a coherent two-level quantum system," *Nature Physics* **15**, 483 (2019).
- [59] R. Bennett, D. Steinbrecht, Y. Gorbachev, and S. Y. Buhmann, "Symmetry Breaking in a Condensate of Light and its Use as a Quantum Sensor," *Phys. Rev. Applied* **13**, 044031 (2020).
- [60] J. Bao, N. Liu, H. Tian, Q. Wang, T. Cui, W. Jiang, S. Zhang, and T. Cao, "Chirality Enhancement Using Fabry-Pérot-Like Cavity," *Research* **2020**, 7873581 (2020).
- [61] Y.-H. Kang, Z.-C. Shi, J. Song, and Y. Xia, "Effective discrimination of chiral molecules in a cavity," *Opt. Lett.* **45**, 4952 (2020).
- [62] X. Zhong, T. Chervy, S. Wang, J. George, A. Thomas, J. A. Hutchison, E. Devaux, C. Genet, and T. W. Ebbesen, "Non-Radiative Energy Transfer Mediated by Hybrid Light-Matter States," *Angew. Chem. Int. Ed.* **55**, 6202 (2016).
- [63] R. Sáez-Blázquez, J. Feist, A. I. Fernández-Domínguez, and F. J. García-Vidal, "Organic polaritons enable local vibrations to drive long-range energy transfer," *Phys. Rev. B* **97**, 241407(R) (2018).

- [64] J. A. Campos, R. F. Ribeiro, and J. Yuen-Zhou, “Resonant catalysis of thermally activated chemical reactions with vibrational polaritons,” *Nature Communications* **10**, 1 (2019).
- [65] J. Lather, P. Bhatt, A. Thomas, T. W. Ebbesen, and J. George, “Cavity Catalysis by Cooperative Vibrational Strong Coupling of Reactant and Solvent Molecules,” *Angew. Chem. Int. Ed.* **58**, 10635 (2019).
- [66] F. Herreral and F. C. Spano, “Dark Vibronic Polaritons and the Spectroscopy of Organic Microcavities,” *Phys. Rev. Lett.* **118**, 223601 (2017).
- [67] T. Neuman and J. Aizpurua, “Origin of the asymmetric light emission from molecular exciton–polaritons” *Optica* **5**, 1247 (2018).
- [68] G. S. Agarwal, *Quantum Optics* (Cambridge University Press, Cambridge, 2013).
- [69] J. Li, X. Zhan, C. Ding, D. Zhang, and Y. Wu, “Enhanced nonlinear optics in coupled optical microcavities with an unbroken and broken parity-time symmetry,” *Phys. Rev. A* **92**, 043830 (2015).
- [70] C. Gardiner and P. Joller, *Quantum Noise* (Springer, Berlin, 2004).
- [71] D. F. Walls and G. J. Milburn, *Quantum Optics*, 2nd ed. (Springer, Berlin, 2008).
- [72] G. S. Agarwal and Y. Zhu, “Photon trapping in cavity quantum electrodynamics,” *Phys. Rev. A* **92**, 023824 (2015).
- [73] R. Culver, A. Lampis, B. Megyeri, K. Pahwa, L. Mudarikwa, M. Holynski, P. W. Courteille, and J. Goldwin, “Collective strong coupling of cold potassium atoms in a ring cavity,” *New J. Phys.* **18**, 113043 (2016).
- [74] S. Kato, N. Német, K. Senga, S. Mizukami, X. Huang, S. Parkins, and T. Aoki, “Observation of dressed states of distant atoms with delocalized photons in coupled-cavities quantum electrodynamics,” *Nature Communications* **10**, 1160 (2019).
- [75] S. Schütz, J. Schachenmayer, D. Hagenmüller, G. K. Brennen, T. Volz, V. Sandoghdar, T. W. Ebbesen, C. Genes, and G. Pupillo, “Ensemble-Induced Strong Light-Matter Coupling of a Single Quantum Emitter,” *Phys. Rev. Lett.* **124**, 113602 (2020).
- [76] M. Tavis and F. W. Cummings, “Exact Solution for an N-Molecule-Radiation-Field Hamiltonian,” *Phys. Rev.* **170**, 379 (1968).
- [77] M. G. Raizen, R. J. Thompson, R. J. Brecha, H. J. Kimble, and H. J. Carmichael, “Normal-mode splitting and linewidth averaging for two-state atoms in an optical cavity,” *Phys. Rev. Lett.* **63**, 240 (1989).
- [78] G. Hernandez, J. Zhang, and Y. Zhu, “Vacuum Rabi splitting and intracavity dark state in a cavity-atom system,” *Phys. Rev. A* **76**, 053814 (2007).
- [79] R. Sawant, O. Dulieu, and S. A. Rangwala, “Detection of ultracold molecules using an optical cavity,” *Phys. Rev. A* **97**, 063405 (2018).